C. 1

NASA TN D-861

NASA TN D-861

TECHNICAL NOTE

D-861

AN APPROXIMATE ANALYSIS OF FILM COOLING ON BLUNT BODIES BY GAS INJECTION NEAR THE STAGNATION POINT

By Byron L. Swenson

Ames Research Center
Moffett Field, Calif.

NATIONAL AERONAUTICS AND SPACE ADMINISTRATION

WASHINGTON September 1961

NATIONAL AERONAUTICS AND SPACE ADMINISTRATION

TECHNICAL NOTE D-861

AN APPROXIMATE ANALYSIS OF FILM COOLING ON BLUNT BODIES BY GAS INJECTION NEAR THE STAGNATION POINT

By Byron L. Swenson

SUMMARY

An approximate method for the estimation of laminar heat transfer to blunt bodies with gaseous film cooling is developed. Attention is focused on the parameters which are important for the design of an attractive heat protection system. Application of the analysis is made to calculate the approximate coolant weight requirement for both a circular and a parabolic entry.

INTRODUCTION

Continued study of heat-protection systems has produced a number of efficient means for dissipating or absorbing the aerodynamic heat otherwise convected to a re-entry vehicle. Among the systems which have shown promise are those based on the injection of foreign gases into the boundary layer of a vehicle. In particular, it is well known and understood that transpiration or normal injection of a foreign gas from a porous wall can efficiently reduce the local heat-transfer rate (see ref. 1). This transpiration method does have some disadvantages, however. First, the injected gas reduces heat transfer primarily in the immediate area of injection and has little influence on heat transfer downstream of this area (ref. 2). In addition, a porous wall presents some structural problems. Since these disadvantages are associated primarily with the method of injection, it seems proper to inquire if other means of injection can be used which are more attractive structurally and which hold promise of providing a larger over-all cooling effect. One such method appears to be the use of gas film cooling. With this method the gas is injected tangentially to the wall and usually from a single port. With tangential injection, mixing of the injected gas is reduced and the gas tends to be maintained in a thin film.

Film cooling has been used to advantage in the heat protection of both wind-tunnel nozzle walls (ref. 3) and blunt re-entry shapes (refs. 4, 5, and 6). In addition, it has been shown that the streamwise gas injection scheme can be used to reduce the skin-friction drag of slender bodies (ref. 7).

For the most part, the previous investigations of film cooling have been experimental in character. While these investigations have indicated attractive features of film cooling, it would seem that the virtues of the method might be further exploited if a simplified analytical treatment of the phenomena were available. These considerations then define the primary objectives of the present paper. The first objective is to obtain an approximate analytic description of film cooling and the second objective is to employ the results of this analysis to determine the design criteria which make the method most attractive.

SYMBOLS

A reference area, ft^2

B distribution parameter

b span width, ft

C_D drag coefficient

c_f skin-friction coefficient

C_i injection coefficient

c_p specific heat at constant pressure, Btu/slug $^{\circ}R$

C_p pressure coefficient

ΔH enthalpy potential, $c_p(T_r - T_w)$, Btu/slug

h heat-transfer coefficient, Btu/ft^2-$^{\circ}R$

I_p drag surface integral

I_s weighted surface area integral

k thermal conductivity, Btu/ft-sec-$^{\circ}R$

$\dot{m}_F$ mass rate of film flow, slugs/sec

m_F total mass of film gas required for protection during entry, slugs

M molecular weight

P body perimeter, ft

p pressure, lb/ft^2

q heating rate, Btu/ft^2-sec

Q integrated heating rate, Btu/sec

r body radial coordinate, ft

R characteristic dimension of body (nose radius), ft

$\overline{R}$ universal gas constant

s arc length along body surface measured from the injection port, ft

T temperature, $^{\circ}R$

t time, sec

t_1 time at which gas film cooling is turned on, sec

t_2 time at which gas film cooling is turned off, sec

u velocity, ft/sec

V vehicle flight velocity, ft/sec

W vehicle weight

Γ_i injection coefficient

δ local body slope, radians

δ_c cone half-angle, deg

δ_w wedge half-angle, deg

μ coefficient of viscosity, slugs/ft-sec

ρ density, slugs/ft^3

Subscripts

o condition of film at point of injection

ı air-film interface

A air

b evaluated at the base

F film

H helium

r recovery condition

s stagnation value

w wall condition

max maximum value encountered during entry

∞ free-stream condition

ANALYSIS

As noted earlier, the following analysis is designed to provide a simple description of film cooling. In keeping with this objective, only laminar flows will be considered and it will be assumed that both the film and air are ideal gases with Prandtl numbers of unity. From the analysis point of view, the problem can be treated in two parts: first, the case where the film is very thin compared to the air boundary layer and, second, the case where the gas film replaces at least the boundary-layer thickness of the air flow. The analysis of the two cases is as follows.

Very Thin Film

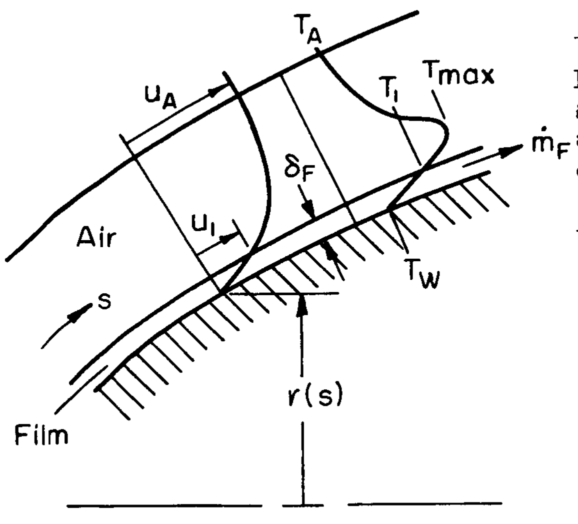

Sketch (a)

Local heating rate.- The thin-film model for film cooling is predicated on the assumption that the gas film is very thin compared to the air boundary layer. This abstraction of the actual boundary-layer flow is shown in sketch (a) where typical velocity and temperature profiles are shown schematically. For simplicity it is assumed that there is no mixing across the air-film interface, or, by implication, that u_1 is the same as existed in the air boundary layer a distance δ_F from the wall without injection. It is also assumed that $u_1 << u_A$.

With the very thin film assumption in mind, the heating rate to the wall can be expressed as follows:

$$q_F \cong k_F \frac{T_1 - T_W}{\delta_F} \tag{1}$$

The thickness of the film can now be established from considerations of the mass flow in the film and the wall shear stress. They are, respectively:

$$\dot{m}_F \cong C\rho_1 u_1 \delta_F P \tag{2}$$

where

$$P = \begin{cases} 2\pi r(s) & \text{axisymmetric flow} \\ b & \text{planar flow} \end{cases}$$

$$C \to \frac{1}{2} \quad \text{as} \quad \delta_F \to 0$$

and

$$\mu_F)_1 \frac{u_1}{\delta_F} \cong \frac{1}{2} \rho_A u_A^2 c_{f_A} \tag{3}$$

Attention is directed for the moment to the viscosity in equation (3). For simplicity it will be assumed that the viscosity may be approximated by $\mu = kT$ where k is the same for all gases. (The accuracy of this approximation is indicated in sketch (b).) This approximation is perhaps best for gases, such as air, helium, nitrogen, and oxygen, and it is poor primarily only for hydrogen. In any event, the approximation is adopted here. Assuming no pressure gradient normal to the wall through the boundary layer we may then write the following:

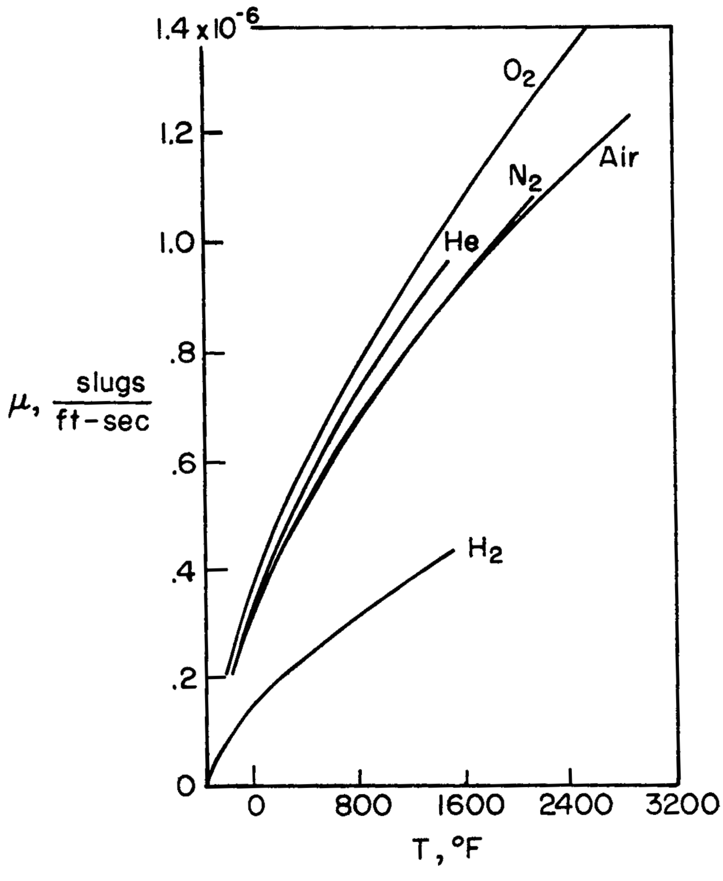

Sketch (b)

$$\frac{\mu_F)_1}{\mu_A} = \frac{T_1}{T_A} = \frac{M_F}{M_A}\frac{\rho_A}{\rho_1} \tag{4}$$

where M is the molecular weight.

Equations (2) and (3) together with equation (4) can now be solved for the film thickness; thus,

$$\delta_F = \frac{T_1}{T_A}\frac{\left(\dfrac{\mu_A \dfrac{M_A}{M_F} \dot{m}_F}{c_{f_A} P}\right)^{1/2}}{\frac{1}{2}\rho_A u_A} \tag{5}$$

Substituting equation (5) into equation (1) using

$$\frac{k_F}{\mu_F)_1 C_{p_F}} = \frac{1}{P_{r_F}} = 1$$

yields

$$q_F = \frac{1}{2}\rho_A u_A c_{f_A} \Delta H_1 \left(\frac{\mu_A P \dfrac{M_F}{M_A}}{\dot{m}_F c_{f_A}}\right)^{1/2} \tag{6}$$

where the enthalpy potential is $\Delta H_1 = c_{p_F}(T_1 - T_w)$. By Reynolds analogy the heating rate without a film is given by:

$$q_A = \frac{1}{2}\rho_A u_A c_{f_A} \Delta H_A$$

therefore,

$$\frac{q_F}{q_A} = \left(\frac{\mu_A P \dfrac{M_F}{M_A}}{\dot{m}_F c_{f_A}}\right)^{1/2} \frac{\Delta H_1}{\Delta H_A} \tag{7}$$

It can be seen from equation (7) that a film of a low molecular weight gas with a low enthalpy potential would reduce the heating rate.

Heating-rate distribution.- The distribution of the cooling effect is determined by a heat balance on the film. With reference again to sketch (a), it is assumed that the amount of heat conducted across the interface is approximately that convected to the wall in the absence of the film. This assumption appears reasonable if $T_1 << T_{max}$. With the additional assumption of an isothermal wall, the heat balance is expressed by:

$$(q_A - q_F)P\, ds \cong \frac{1}{2}\dot{m}_F\, d\Delta H_1$$

The result can be rewritten into the following form with the assumption that for blunt bodies in hypersonic flow ΔH_A is constant over the body;

$$\left(1 - \frac{q_F}{q_A}\right)\frac{q_A}{q_{A,s}}\frac{P}{R}\, d\,\frac{s}{R} = \frac{\dot{m}_F\Delta H_A}{2q_{A,s}R^2}\, d\,\frac{\Delta H_1}{\Delta H_A} \tag{8}$$

where R is a characteristic length of the body (say the nose radius). The heating-rate distribution is now determined as a function of body shape, mass rate of injection, and flight conditions by solution of the linear differential equation resulting from the combination of equations (7) and (8).

$$\frac{d(\Delta H_1/\Delta H_A)}{d(s/R)} + \frac{2q_{A,s}R^2}{\dot{m}_F\Delta H_A}\beta\frac{q_A}{q_{A,s}}\frac{P}{R}\frac{\Delta H_1}{\Delta H_A} = \frac{2q_{A,s}R^2}{\dot{m}_F\Delta H_A}\frac{q_A}{q_{A,s}}\frac{P}{R}$$

The solution is as follows:

$$\frac{q_F}{q_A} = \frac{\beta}{E(s/R)}\left[\left(\frac{\Delta H_1}{\Delta H_A}\right)_o + F\left(\frac{s}{R}\right)\right] \tag{9}$$

where

$$\beta = \left[\frac{\mu_A P(M_F/M_A)}{\dot{m}_F c_{f_A}}\right]^{1/2} = \left[\frac{(M_F/M_A)\Delta H_A}{2\dot{m}_F q_{A,s}}\,\frac{\mu_A\rho_A u_A P}{q_A/q_{A,s}}\right]^{1/2}$$

$$E\left(\frac{s}{R}\right) = \exp\left(\frac{2q_{A,s}R^2}{\dot{m}_F\Delta H_A}\int_o^{s/R}\beta\frac{q_A}{q_{A,s}}\frac{P}{R}\,d\zeta\right)$$

$$F\left(\frac{s}{R}\right) = \frac{2q_{A,s}R^2}{\dot{m}_F\Delta H_A}\int_o^{s/R}E(\xi)\frac{q_A}{q_{A,s}}\frac{P}{R}\,d\xi$$

and $\Delta H_1/\Delta H_A$ is the enthalpy-potential ratio at the injection point.

The parameter β can be given physical significance if the equation for the film thickness (i.e., eq. (5)) is rewritten in terms of β.

$$\delta_F = \mu_A \frac{T_1}{T_A} \frac{u_1}{(1/2)\rho_A u_A{}^2 c_{f_A}} \frac{u_A/u_1}{\beta}$$

or

$$\mu_F)_1 \frac{u_1}{\delta_F} = \frac{1}{2} \rho_A u_A{}^2 c_{f_A} \frac{\beta}{u_A/u_1}$$

Comparison of this result with equation (3) shows that β can be interpreted as

$$\beta \cong u_A/u_1$$

Since it is necessary that u_A/u_1 be much greater than 1 to satisfy the approximations of the analysis, it follows that $\beta >> 1$ is a requisite of the analysis. It also follows that a restriction must be imposed on the mass flow in the film so that $\beta >> 1$ is satisfied; that is,

$$\dot{m}_F << \frac{\mu_A P(M_F/M_A)}{c_{f_A}} = \frac{(M_F/M_A)\Delta H_A}{2q_{A,s}} \frac{\mu_A \rho_A u_A P}{q_A/q_{A,s}} \tag{10}$$

The results obtained from equation (9) for film mass flows in excess of the above restriction will be questionable since this condition will violate the basic equations of the analysis - in particular, equation (3).

Integrated heating rate.- The heating rate integrated over the body can not be obtained in closed form for this type of film flow. However, it may be obtained by graphical integration of equation (9).

Thick Film

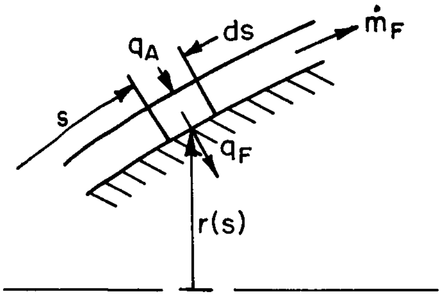

Sketch (c)

Local heating rate.- The basic assumption of the thick-film model of film cooling is that the gas film replaces at least the boundary-layer flow of the air. Again mixing across the air-film interface will be assumed small, being only on a molecular scale. This abstraction of the flow is shown schematically in sketch (c). It is obvious that there can be no pressure difference across the interface and that the assumption of small mixing requires that at the interface, the velocities of the air and the gas film be equal.

With these points in mind, the ratio of the local heating rate with film cooling to that without can be written as

$$\frac{q_F}{q_A} = \frac{h_F}{h_A} \frac{(T_r - T_w)_F}{(T_r - T_w)_A} \tag{11}$$

Also, by Reynolds analogy, the ratio of the heat-transfer coefficients is

$$\frac{h_F}{h_A} = \frac{(\rho u c_f c_p)_F}{(\rho u c_f c_p)_A} \tag{12}$$

Combining equations (11) and (12) yields the following expression:

$$\frac{q_F}{q_A} = \frac{(\rho u c_f)_F \Delta H_F}{(\rho u c_f)_A \Delta H_A} \tag{13}$$

where

$$\Delta H = c_p(T_r - T_w)$$

The densities in equation (13) are evaluated with the equation of state

$$p = \rho \frac{\bar{R}}{M} T$$

where $\bar{R}$ is the universal gas constant. With this result and with the previously noted conditions, that is, $u_F/u_A = 1$ and $p_F/p_A = 1$, equation (13) becomes

$$\frac{q_F}{q_A} = \frac{M_F}{M_A} \frac{T_A}{T_F} \frac{c_{f_F}}{c_{f_A}} \frac{\Delta H_F}{\Delta H_A} \tag{14}$$

Attention is now directed to the ratio of skin-friction coefficients. This ratio was evaluated in reference 7 for the special case of a helium film. The result of reference 7 can be generalized to other gases if the use is again made of the approximation that viscosity may be written $\mu = kT$ where k is the same for all gases. Finally, since the skin-friction coefficient is inversely proportional to the square root of the Reynolds number, the following ratio is obtained:

$$\frac{c_{f_F}}{c_{f_A}} = \frac{T_F}{T_A}\sqrt{\frac{M_A}{M_F}} \tag{15}$$

Substitution of equation (15) into equation (14) yields:

$$\frac{q_F}{q_A} = \sqrt{\frac{M_F}{M_A}}\frac{\Delta H_F}{\Delta H_A} \tag{16}$$

From equation (16), it is again seen, as in the previous flow model, that low heating rates will be obtained with a film of gas having a low molecular weight and a low enthalpy potential.

Heating-rate distribution.- With the ratio of local heating rates determined, consideration must now be given to the distribution of heating rates over a body with film cooling. To obtain this distribution, it is necessary to evaluate the enthalpy potential of the film, ΔH_F. The potential increases as the film flows aft over the body as a result of the absorption of heat by the film. As the enthalpy potential increases so does the ability of the film to convect heat to the wall.

A limiting estimate of the distribution of the enthalpy potential of the film is immediately evident. The simplest assumption is that the enthalpy potential of the film does not change as it flows around the body. This would occur if the film not only replaced the boundary layer but was sufficiently thick that conduction and diffusion of heat from the exterior air did not penetrate to the boundary layer by the time the film flowed off the rear of the body. In this case, equation (16) would completely describe the heating-rate distribution about the body since ΔH_F would be constant at the value for injection. Unfortunately this condition will not often exist in practice, especially for axisymmetrical bodies where the film generally will thin greatly as it flows aft.

Integrated heating rate.- In the case of a thick film it is easy to determine the integrated heating rate or integral of the heat rate over the body surface. The heat accepted per unit time is

$$Q = \int_0^{s_b} qP\,ds$$

where s_b is the arc length to the base of the body. It is easily shown that the ratio of the integrated heat rate with film cooling to that without can be written as

$$\frac{Q_F}{Q_A} = \sqrt{\frac{M_F}{M_A} \frac{\Delta H_{F,o}}{\Delta H_A}} \tag{17}$$

The term $\Delta H_{F,o}$ is the enthalpy potential of the film at the injection point.

Intermediate Film Model

A third possible model of the film flow has characteristics somewhat intermediate to those of the two models already considered. With this model, it is assumed that the film replaces just the boundary-layer thickness of the air flow.

Local heating rate.- With this model, the local heating rate is again given by equation (16). The difference between this model and the previous one lies in the amount of heat transported across the air-film interface and, hence, in the distribution of heating rate.

Heating-rate distribution.- A limiting condition on the amount of heat transported (i.e., by diffusion and conduction) to the film from the exterior air across the interface is that it is the same as that convected to the body in the absence of a film. At first glance, this assumption appears to be contradictory to that used to develop equation (16). However, it is felt that, especially when a large potential exists between the film and free-stream conditions, the conduction across the interface could be of the same order as the convective heat transfer. It should be noted that a similar assumption was employed by the authors of reference 8 to obtain a correlation of recovery temperature for film-cooled walls. This assumption appears to be conservative in the sense that less heat will probably cross the interface; but this does not mean that the entire analysis is conservative. There are effects not considered here, such as mixing and diffusion, that may have a detrimental effect on the cooling provided by the film. In any event, due to the simplicity gained from this assumption, it will be adopted here.

A heat balance of the film based on these considerations is given by the following.

$$(q_A - q_F)P\ ds = \dot{m}_F\ d(\Delta H_F) \tag{18}$$

Equation (18) can be rewritten in the following form with the assumption that ΔH_A is constant over the body.

$$\left(1 - \frac{q_F}{q_A}\right) \frac{q_A}{q_{A,s}} \frac{P}{R}\ d\ \frac{s}{R} = \frac{\dot{m}_F \Delta H_A}{q_{A,s} R^2}\ d\ \frac{\Delta H_F}{\Delta H_A} \tag{19}$$

The heating-rate distribution with film injection can now be determined as a function of body shape, mass rate of injection, and flight conditions by the solution of the linear differential equation resulting from the combination of equations (16) and (19).

$$\frac{d\left(\frac{\Delta H_F}{\Delta H_A}\right)}{d\left(\frac{s}{R}\right)} + \frac{\sqrt{\frac{M_F}{M_A}}\, q_{A,s}R^2}{\dot{m}_F \Delta H_A} \frac{q_A}{q_{A,s}} \frac{P}{R} \frac{\Delta H_F}{\Delta H_A} = \frac{q_{A,s}R^2}{\dot{m}_F \Delta H_A} \frac{q_A}{q_{A,s}} \frac{P}{R}$$

The solution is as follows:

$$\frac{q_F}{q_A} = 1 - \left(1 - \sqrt{\frac{M_F}{M_A}} \frac{\Delta H_{F,o}}{\Delta H_A}\right) e^{-B} \tag{20}$$

where

$$B = \frac{\sqrt{\frac{M_F}{M_A}}\, q_{A,s}R^2}{\dot{m}_F \Delta H_A} I_s\left(\frac{s}{R}\right)$$

and

$$I_s\left(\frac{s}{R}\right) = \int_o^{s/R} \frac{q_A}{q_{A,s}} \frac{P}{R}\, d\,\frac{s}{R}$$

The term $\Delta H_{F,o}$ is the enthalpy potential of the film at the injection point. Since

$$1 - \sqrt{\frac{M_F}{M_A}} \cdot \frac{\Delta H_{F,o}}{\Delta H_A} = \left(1 - \frac{q_F}{q_A}\right)_o$$

equation (20) can be placed in a more symmetrical form

$$\frac{1 - (q_F/q_A)}{[1 - (q_F/q_A)]_o} = e^{-B} \tag{21}$$

In the discussion that follows, the term $[1 - (q_F/q_A)]_o$ will be called the injection parameter and the term B, the distribution parameter. In addition, the integral I_s may be thought of as surface-area integral, weighted as to heating rate.

Integrated heating rate.- In the case of the intermediate-film model it is again easy to determine the integrated heating rate or integral of the heat rate over the body surface. This integral helps define the total heat load accepted by the body. The heat accepted per unit time is again

$$Q = \int_0^{s_b} qP \, ds$$

Therefore, the ratio of the integrated heat rate with film cooling to that without can be written:

$$\frac{Q_F}{Q_A} = \frac{\displaystyle\int_0^{s_b/R} \frac{q_F}{q_A} \frac{q_A}{q_{A,s}} \frac{P}{R} \, d \, \frac{s}{R}}{\displaystyle\int_0^{s_b/R} \frac{q_A}{q_{A,s}} \frac{P}{R} \, d \, \frac{s}{R}}$$

or

$$\frac{Q_F}{Q_A} = \frac{\displaystyle\int_0^{I_s(s_b/R)} \frac{q_F}{q_A} (I_s) dI_s}{I_s(s_b/R)} \tag{22}$$

Substituting equation (20) into equation (22) and integrating yields

$$1 - \frac{Q_F}{Q_A} = \left(1 - \frac{q_F}{q_A}\right)_o \frac{1 - e^{-B_b}}{B_b} \tag{23}$$

where B_b is evaluated at the base and is

$$B_b = \frac{\sqrt{\frac{M_F}{M_A} q_{A,s} R^2 I_s \frac{s_b}{R}}}{\dot{m}_F \Delta H_A}$$

RESULTS AND DISCUSSION

Comparisons With Existing Experimental Data

In an attempt to assess the accuracy of the present analyses, comparisons will be made with existing experimental data for the effects of film injection on heat transfer. Some of the available data on film cooling are presented in reference 4 where results were obtained with both helium and nitrogen as the injected gas. For these gases results are presented in the form of the integrated heating rate to a hemispherical nose for segments extending 30°, 60°, and 80° from the stagnation point. These experimental results are presented as a function of the injection coefficient, C_i, in figures 1 and 2.

Additional data on film cooling for the case of air injection are obtainable from reference 6. Again, only integrated heating rates to a full hemisphere were obtained. For the purposes of comparison with the results of the present analysis, the data of reference 6 have been converted from the mean heat-transfer coefficients presented to the form of integrated heating rates. This conversion has been made first with the use of the measured recovery and wall temperatures and secondly with the use of the measured recovery temperatures and assuming a cold wall. The latter conversion, of course, assumes that the measured heat-transfer coefficients are independent of wall temperature. It should be noted that the approximations made in the analysis will be most closely satisfied when a large potential exists between the wall and the free-stream recovery conditions. Since the data of reference 6 were obtained with the use of a heated model with a small temperature potential between the wall and free-stream recovery conditions, it seemed necessary to adjust the data of cold wall conditions before comparing them with the results of the analysis. The data from reference 6 are shown in figure 3.

For each set of data, comparisons are made with the results of each of the present analyses. The theoretical estimates shown in figures 1, 2, and 3 were obtained with equations (9), (17), and (23). In each application of the thin-film analysis it was found that the restriction placed on this analysis, as given by equation (10), was seriously violated. Typical values of β were about 1/4, indicating that the velocity at the film-air interface was four times the local free-stream velocity. It is suggested, therefore, that for the available experimental results, the mass flows were too great to permit valid use of this analysis. For this reason, the reasonable agreement obtained in some cases between the results of this particular analysis and the experimental data must be viewed with some reservations.

Perhaps the most obvious conclusion from the comparisons shown in figures 1, 2, and 3 is that the thick-film analysis is the least accurate. Apparently this analysis does not represent the film-cooling phenomena except as a limit as the mass flow becomes very large.

The results obtained with the intermediate model appear to represent a reasonable approximation for most of the experimental data. Detailed examination of the three sets of data indicates some inconsistencies, however. The helium-injection data of reference 4 seem to be quantitatively predicted, at least at the lower injection rates, by equation (23). The trend of the data of reference 6, when adjusted to cold-wall conditions, is also predicted by this equation. On the other hand, the nitrogen-injection data of reference 4 disagree with equation (23) of the analysis. Essentially no reduction in heating rate was measured in reference 4 at the lower injection rates. It should be noted that this result is not in agreement with the results of reference 6 for a gas of approximately the same molecular weight.

In any event, it would appear that the available data do not permit any definite conclusion as to the accuracy of the present analysis. Real justification of the analysis and the conclusions gained from it will have to wait for additional and more comprehensive film-cooling data. In spite of this restriction, further considerations of the application of film cooling are warranted. For these further considerations, attention will be restricted to the intermediate-film model. This model will be used since it is at least as accurate as the others; it is not subject to the reservations attached to the thin-film model; and it is somewhat more simple in form.

Applications of the Analysis

Injection coefficient.- With the dependent effects of film injection defined in the analysis presented earlier, attention at this point is turned to the independent variable, the rate of injection. In most studies, for the purposes of scaling, the rate of injection has been described in terms of an injection coefficient, C_i, which may be written as

$$C_i = \frac{\dot{m}_F}{\rho_\infty u_\infty \pi R^2}$$

This coefficient refers the injection rate to the rate at which free-stream air is swept out by an area of radius, R. While this coefficient is convenient, it holds no true physical significance. The results of the analysis of the intermediate-flow model suggest the use of another coefficient of injection which appears as a component of the parameter, B:

$$\Gamma_i = \frac{\dot{m}_F}{(q_{A,s}/\Delta H_A)R^2} \tag{24}$$

When this coefficient is used, the rate of injection, $\dot{m}_F$, is referenced to mass rate of coolant it would take to absorb the heat convected to a stagnation area of R^2 if that mass were increased in enthalpy by an amount equal to ΔH_A.[1] For this reason, the coefficient Γ_i would seem to have greater significance for correlations than does C_i. Thus the distribution parameter, B, may be written as

$$B = \frac{\sqrt{\frac{M_F}{M_A}}\, I_s}{\Gamma_i} \tag{25}$$

Coolant requirements.- The total weight of film coolant used during a given flight may be written

$$m_F = \int_t \dot{m}_F \, dt$$

where this equation is integrated over the time of flight. In terms of the injection coefficient, Γ_i, this equation is

$$m_F = R^2 \int_t \frac{q_{A,s}}{\Delta H_A} \Gamma_i \, dt \tag{26a}$$

or in terms of the distribution parameter, B, it is

$$m_F = \sqrt{\frac{M_F}{M_A}}\, R^2 I_s \left(\frac{s_b}{R}\right) \int_t \frac{q_{A,s}}{\Delta H_A B} \, dt \tag{26b}$$

It is assumed in equation (26b) that for hypersonic flight conditions, the ratio $q_A/q_{A,s}$ is independent of Mach number and thus I_s is not a function of time.

Film injection may be applied to provide cooling in several different ways. For example, it may be desirable to inject in such a way as to keep the integral of the heating rate over the body at some constant fraction of that with no injection during the entire flight. For this case and for $\Delta H_{F,o} << \Delta H_A$ then Γ_i or B is a constant (see eq. (23)) and not a function of time. Therefore,

---

[1]Note that the reference mass rate differs by a factor from the mass rate of coolant it would take to absorb all the heat normally transmitted to the body if that mass were increased in enthalpy by ΔH_A. The factor is $I_s(s_b/R)$.

$$m_F = R^2\Gamma_i \int_0^t \frac{q_{A,s}}{\Delta H_A}\,dt$$

In some cases it might also be desirable to inject in such a way as to keep the local heating rate at any point on the body below a certain design limit. In this case then, equations (21) and (25) must be used together with the known heating-rate distribution of the body without injection to determine how Γ_i should vary with time along the flight trajectory. The total mass can then be calculated by the use of either equation (26a) or (26b).

Another possible application of film cooling might be to keep the integrated heat rate below a certain design limit. Consider, for example, an $L/D = 0$ entry with an integrated heat rate as a function of time as shown in sketch (d). Consider now a structure with a certain design integrated heating rate, Q_D, that it can withstand or dissipate without assistance. Obviously optimum performance of the heat protection system is attained ideally when the structure is used to its fullest capacity. Therefore, the film-cooling system would not be turned on until time t_1 and then would be controlled in such a way that $Q_F = Q_D$ until time t_2 when the heating rate Q_A would again become equal to Q_D.

To keep Q_F equal to Q_D during the time interval t_1 to t_2 it is necessary to control the mass rate of injection (and hence B) as indicated below. From equation (23)

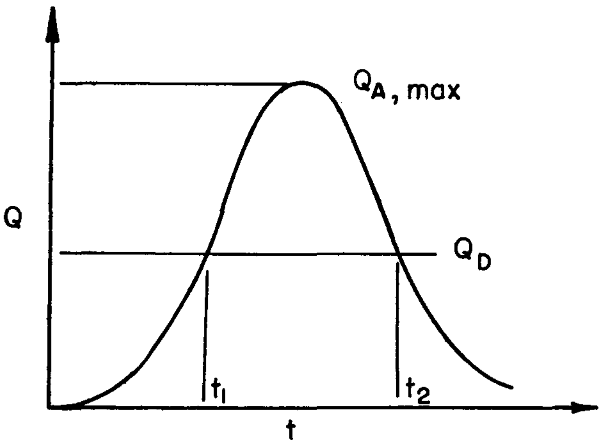

Sketch (d)

$$\frac{Q_F}{Q_A} = \frac{Q_D}{Q_A} = 1 - \left(1 - \frac{q_F}{q_A}\right)_o \frac{1 - e^{-B_b}}{B_b}$$

Consider now injecting the film so that $\Delta H_{F,o} = 0$; then the parameter

$$\left(1 - \frac{q_F}{q_A}\right)_o = 1$$

thus

$$\frac{B_b(t)}{1 - e^{-B_b(t)}} = \frac{Q_A(t)}{Q_A(t) - Q_D} \tag{27}$$

A graph of the left side of equation (27) is shown in sketch (e). Suppose that for example $Q_D = (1/2)Q_{A,max}$, then B_b must vary over the period t_1 to t_2 as shown by the arrows in sketch (e). It is easy to see that during this variation of B_b,

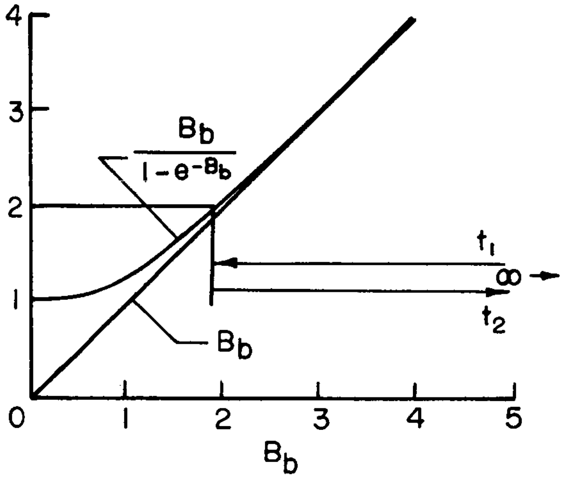

Sketch (e)

$$\frac{B_b}{1 - e^{-B_b}} \cong B_b$$

Thus we may write (noting that $q_{A,s}R^2I_s = Q_A$):

$$B_b(t) = \frac{\sqrt{\frac{M_F}{M_A}}\, Q_A(t)}{\dot{m}_F(t)\Delta H_A(t)} \cong \frac{Q_A(t)}{Q_A(t) - Q_D} \tag{28}$$

or that

$$\dot{m}_F(t) \cong \sqrt{\frac{M_F}{M_A}}\, \frac{Q_A(t) - Q_D}{\Delta H_A(t)} \tag{29}$$

Equation (29) can be now rewritten in the form

$$\dot{m}_F(t) \cong \sqrt{\frac{M_F}{M_A}}\, R^2 I_s \left(\frac{s_b}{R}\right) \frac{q_{A,s}(t)}{\Delta H_A(t)} \left[1 - \frac{Q_D}{Q_A(t)}\right] \tag{30}$$

or the total coolant mass required is

$$m_F = \sqrt{\frac{M_F}{M_A}}\, R^2 I_s \left(\frac{s_b}{R}\right) \int_{t_1}^{t_2} \frac{q_{A,s}}{\Delta H_A} \left(1 - \frac{Q_D}{Q_A}\right) dt \tag{31}$$

These are not the only ways in which the coolant injection might be controlled during given flight conditions. It is usually easy to determine how the distribution parameter B, and hence the mass rate of injection, must vary with time for the particular application under consideration. Then either equation (26a) or equation (26b) can be used to calculate the total mass of coolant required.

Design Parameters

Let us now inquire what information can be obtained from the intermediate-film model as to the nature of the film and body shape which will provide the heat-protection system with the best performance. Attention will be given first to the most attractive type of film.

Injection parameter.- The present analysis indicates that the reduction in local and integrated heating rates is directly proportional to the injection parameter

$$\left(1 - \frac{q_F}{q_A}\right)_o = 1 - \sqrt{\frac{M_F}{M_A}} \frac{\Delta H_{F,o}}{\Delta H_A}$$

It can be seen from this result that the cooling effect of the film increases with decreasing molecular weight, M_F, and with decreasing enthalpy potential, $\Delta H_{F,o}$, of the injected gas. Thus a light-weight gas injected at low temperature would appear to be most attractive for use in film cooling. This result is, of course, in agreement with the conclusions reached in previous studies of the effects of film injection (see, e.g., refs. 3, 4, 5, and 7). The body shapes which appear attractive for film cooling are, in part, dictated by consideration of the cooling distribution.

Distribution parameter.- The distribution of the local and integrated heating rates provided by film injection depends upon the distribution parameter, B, where

$$B = \frac{\sqrt{M_F/M_A}\, q_{A,s} R^2 I_s}{\dot{m}_F \Delta H_A}$$

This dependence is defined by equations (21) and (23) and is shown graphically in figure 4. It is apparent from figure 4 that from the heating standpoint a small value of the distribution parameter B is desirable. Again it can easily be seen that, consistent with the previous finding, it is desirable to use a low molecular weight gas. However, for given flight conditions, vehicle and injected gas, a low value of B implies a high injection mass-flow rate, and hence an increase in the weight of coolant required. Thus, it is apparent that the vehicle must be designed to keep the mass-flow rates low and still keep B small. This can be attained to some extent through control of the shape parameters I_s and R. Consider first the weighted surface-area integral I_s.

It is recalled that this integral is defined as follows:

$$I_s\left(\frac{s}{R}\right) = \int_0^{s/R} \frac{q_A}{q_{A,s}} \frac{P}{R} \, d \frac{s}{R}$$

Calculations have been made of the values of I_s for hypersonic flows about both cylindrically blunted wedges and spherically blunted cones. The results are shown in figures 5 and 6, respectively. The theory of Lees (ref. 9) was used to obtain the heating-rate distribution for both planar and axisymmetric flows.[2] The parameter b appearing in the planar case (i.e., fig. 5) is the span width.

The results presented in figures 5 and 6 tend to indicate that bodies with relatively small wedge or cone angles will have the lowest values of I_s. In any direct comparison, however, it is necessary to hold some physical property of the bodies constant. The following discussion illustrates how such comparisons might be made.

It has been shown (see, e.g., eq. (26b)) that the required mass of film coolant for various types of operation is proportional to:

$$m_F \propto R^2 I_s \int_t \frac{q_{A,s}}{\Delta H_A} \, dt \tag{32}$$

Now, consider for example an atmospheric entry at given entrance velocity, lift-drag ratio, and entrance angle. It can be shown that

$$\frac{q_{A,s}}{\Delta H_A} \propto \left(\frac{W}{C_D A R}\right)^{1/2}$$

or for a given over-all vehicle density

$$\frac{q_{A,s}}{\Delta H_A} \propto \left(\frac{Vol}{C_D A R}\right)^{1/2} \tag{33}$$

---

[2]Lees has also shown in reference 10 that the distribution for planar flow differs from that for axisymmetric flow by only a few percent.

It is now possible to define a drag-surface integral under hypersonic flight conditions so that

$$C_D A \equiv R^2 I_p \left(\frac{s_b}{R}\right) \tag{34}$$

where

$$I_p\left(\frac{s_b}{R}\right) = \int_0^{s_b/R} C_p \frac{P}{R} \sin \delta \, d\,\frac{s}{R}$$

and where δ is the local slope of the body. Calculations have been made of the variation of I_p with s/R for spherically blunted cones. Pressure coefficients obtained with Newtonian impact theory were used (i.e., $C_p = 2 \sin^2\delta$) and the results are shown in figure 7.

From equations (32), (33), and (34) it is possible to write the following:

$$m_F \propto (\mathrm{Vol})^{1/2} R^{1/2} \frac{I_s}{I_p^{1/2}}$$

Thus for vehicles of the same volume, the one with the lowest value of $R^{1/2}(I_s/I_p^{1/2})$ will require the lowest weight of coolant.

From the information supplied by figures 6 and 7, the variation of the parameter $R^{1/2}(I_s/I_p^{1/2})$ with nose radius R has been calculated for spherically blunted cones with a volume equal to 50 cubic feet. The results are shown in figure 8. The curve labeled "Spherical Segment" is the limiting envelope where all the volume (50 cu ft) is contained in the spherical segment of the nose. For this example case at least, it is indicated that certain body shapes require less coolant than others. In particular, for bodies with small nose radii, small cone angles appear to have advantages for use with film cooling.

Illustrative Examples

To illustrate more graphically the effect of film cooling on the heat transfer to blunt bodies and to show additionally the relative importance of the parameters derived in the analysis, several example cases have been calculated.

Fixed flight conditions.- In the first example, a blunted cone with a half-angle of 30° and a spherical nose of 1-foot radius was considered to be flying at an altitude of 200,000 feet and at a velocity of 16,000 feet per second. The stagnation heating rate is then about 70 Btu/ft^2-sec. The heating-rate distributions over the body for various amounts of helium film injection are shown in figure 9(a). In each case, the helium is assumed to be injected at or very near the stagnation point with an injection parameter, $(1 - \sqrt{M_F/M_A}\ \Delta H_{F,o}/\Delta H_A) = 1$. It should be remembered that these curves are for very particular flight conditions and body shape and are only indicative of the distributions obtained with film cooling. With this restriction in mind, it is noted that within the framework of the analysis, the injection of sufficient helium can have a very pronounced effect on the heating-rate distribution and that the cooling may be effective several nose radii downstream of the point of injection.

The effect on the heating-rate distribution of changes in the injection parameter $(1 - \sqrt{M_F/M_A}\ \Delta H_{F,o}/\Delta H_A)$ can be seen in figure 9(b). Here the same flight conditions and body shape are assumed as in the previous case shown in figure 9(a). In this case, however, a constant mass rate of injection of helium is assumed at 10^{-3} slug/sec. Heating distributions with various values of the injection parameter are shown. It can be seen that the heating-rate distribution returns to that with no injection as the injection parameter $(1 - \sqrt{M_F/M_A}\ \Delta H_{F,o}/\Delta H_A)$ approaches zero (i.e., as $\Delta H_{F,o}$ is increased).

Nose radius is also an important parameter, as discussed earlier. Changes in nose radius produce two effects on the distribution parameter B. An increase in nose radius increases the surface area but also decreases the stagnation point heating rate. Some of these effects of nose radius on the heating-rate distribution are illustrated in figure 9(c). Again the same flight conditions were used as in the previous examples. An injection parameter of 1.0 and a mass rate of helium injection of 10^{-3} slugs/sec are also assumed. Results for various nose radii are shown. The injection has the largest effect for the bodies with the smallest nose radii. In this case, the primary effect is that (with the larger nose radii) a given mass rate of injection must cover a larger surface area and is thus less effective downstream of the injection point.

Application to atmosphere entry.- Other examples have also been calculated to evaluate more clearly the use of film cooling for heat protection during atmosphere entry. The vehicle considered in these calculations is shaped similar to the Mercury capsule and is shown in figure 10. In these examples two entry trajectories for nonlifting vehicles, one from circular satellite orbit, and one from a parabolic orbit with a maximum deceleration of 8 g were considered. The vehicle characteristics used are summarized in the following table.

Entry	W	R	W/C_DA	I_s
Circular	2500 lb	7 ft	36.5 lb/ft^2	0.77
Parabolic	4000 lb	10 ft	28.5 lb/ft^2	.77

The normalized heating rate and velocity histories for the entries under consideration were obtained with the aid of reference 11 and are shown in figure 11. Only front face heating will be considered.

It is suggested that film cooling should be used in connection with and as a complement to other means of heat protection. In this way the flexibility and possibly the efficiency of the over-all heat protection system can be improved. To illustrate this point consider a beryllium heat sink protecting the described vehicles entering along the described trajectories. The approximate total weights of heat-sink material required for protection under these conditions are shown in the following table:

Entry	Weight of heat sink, lb
Circular	360
Parabolic	1050

The injection of helium can be used in conjunction with a heat sink of reduced weight. In the present examples it was considered that the helium was injected in such a way as to keep the integrated heating rate accepted by the vehicle at one-half the value existing without injection during the entire entry. Thus the total heat load for an entry is reduced by one-half. From figure 4, this reduction requires, for an injection parameter of unity, a distributional parameter, B, of 1.60. Thus the mass of helium required is

$$m_F = \frac{\sqrt{\dfrac{M_F}{M_A}}\, R^2 I_s}{B} \int_t \frac{q_{A,s}}{\Delta H_A}\, dt$$

$$m_F = \frac{\sqrt{\dfrac{M_F}{M_A}}\, R^2 I_s}{1.60} \int_t \frac{q_{A,s}}{\Delta H_A}\, dt$$

Since the entry heat load is reduced by one-half, the amount of heat-sink material required is also reduced by one-half. Accordingly, the results of the calculations for the example trajectories give the following total weights for the heat-protection system.

Entry	Weight of heat sink	Weight of helium
Circular	180 lb	12.5 lb
Parabolic	525 lb	22.5 lb

The apparent weight savings due to helium injection are not as large as might be indicated by these numbers. Additional weight is required by the system for tankage and for flow regulation which may be as high as an order of magnitude greater than the helium weight.

CONCLUDING REMARKS

A simple method for the estimation of heating rates to blunt shapes with film cooling has been developed. The method indicates that the primary requirement of film cooling is the replacement of the high-enthalpy boundary layer with a low-enthalpy film. As this film flows along a body, the heat convected to the body increases somewhat as a result of an increase in enthalpy from the absorption of part of the convective heat transfer by the film. Results obtained with the method were compared with existing experimental data. Unfortunately, no real conclusions could be made as to the accuracy of the analysis in predicting the cooling effect of film injection. The method was also used to indicate some of the important parameters for the attractive performance of a film-cooling system. It was found that (1) the molecular weight of the film gas should be low, and (2) the enthalpy potential of the film should be small.

Application of the analysis was also made to the calculation of the weight of a heat protection system utilizing helium film cooling in combination with a beryllium heat sink. This calculation was made for a vehicle shaped after the Mercury capsule concept and for nonlifting entries from circular and parabolic speeds. The results of these calculations were compared to the weights of a simple, all-beryllium heat sink. A significant weight saving was indicated.

Ames Research Center
National Aeronautics and Space Administration
Moffett Field, Calif., March 28, 1961

REFERENCES

1. Pappas, C. C.: Effect on Injection of Foreign Gases on the Skin Friction and Heat Transfer of the Turbulent Boundary Layer. IAS Rep. No. 59-79.

2. Chung, Paul M.: Effect of Localized Mass Transfer Near the Stagnation Region of Blunt Bodies in Hypersonic Flight. NASA TN D-141, 1960.

3. Ferri, Antonio, and Libby, Paul A.: The Use of Helium for Cooling Nozzles Exposed to High Temperature Gas Streams. WADC TN 55-318, Mar. 1956.

4. McMahon, Howard M.: An Experimental Study of the Effect of Mass Injection at the Stagnation Point of a Blunt Body. GALCIT Hypersonic Research Memorandum 42, May 1, 1958.

5. Warren, C., and Hugh E.: An Experimental Investigation of the Effect of Ejecting a Coolant Gas at the Nose of a Blunt Body. GALCIT Hypersonic Research Project 47, Dec. 15, 1958.

6. Stalder, Jackson R., and Inouye, Mamoru: A Method of Reducing Heat Transfer to Blunt Bodies by Air Injection. NACA RM A56B27a, 1956.

7. Swenson, Byron L.: An Exploratory Study of the Reduction in Friction Drag Due to Streamwise Injection of Helium. NASA TN D-342, 1961.

8. Hatch, James E., and Papell, S. Stephen: Use of a Theoretical Flow Model to Correlate Data for Film Cooling or Heating an Adiabatic Wall by Tangential Injection of Gases of Different Fluid Properties. NASA TN D-130, 1959.

9. Lees, L.: Laminar Heat Transfer Over Blunt-Nosed Bodies at Hypersonic Flight Speeds. Jet Propulsion, April 1956, pp. 259-269.

10. Lees, L.: Hypersonic Flow. IAS Preprint No. 554, June 1955.

11. Nielsen, Jack N., Goodwin, Frederick K., and Mersman, William A.: Three-Dimensional Orbits of Earth Satellites, Including Effects of Earth Oblateness and Atmospheric Rotation. NASA MEMO 12-4-58A, 1958.

Page intentionally left blank

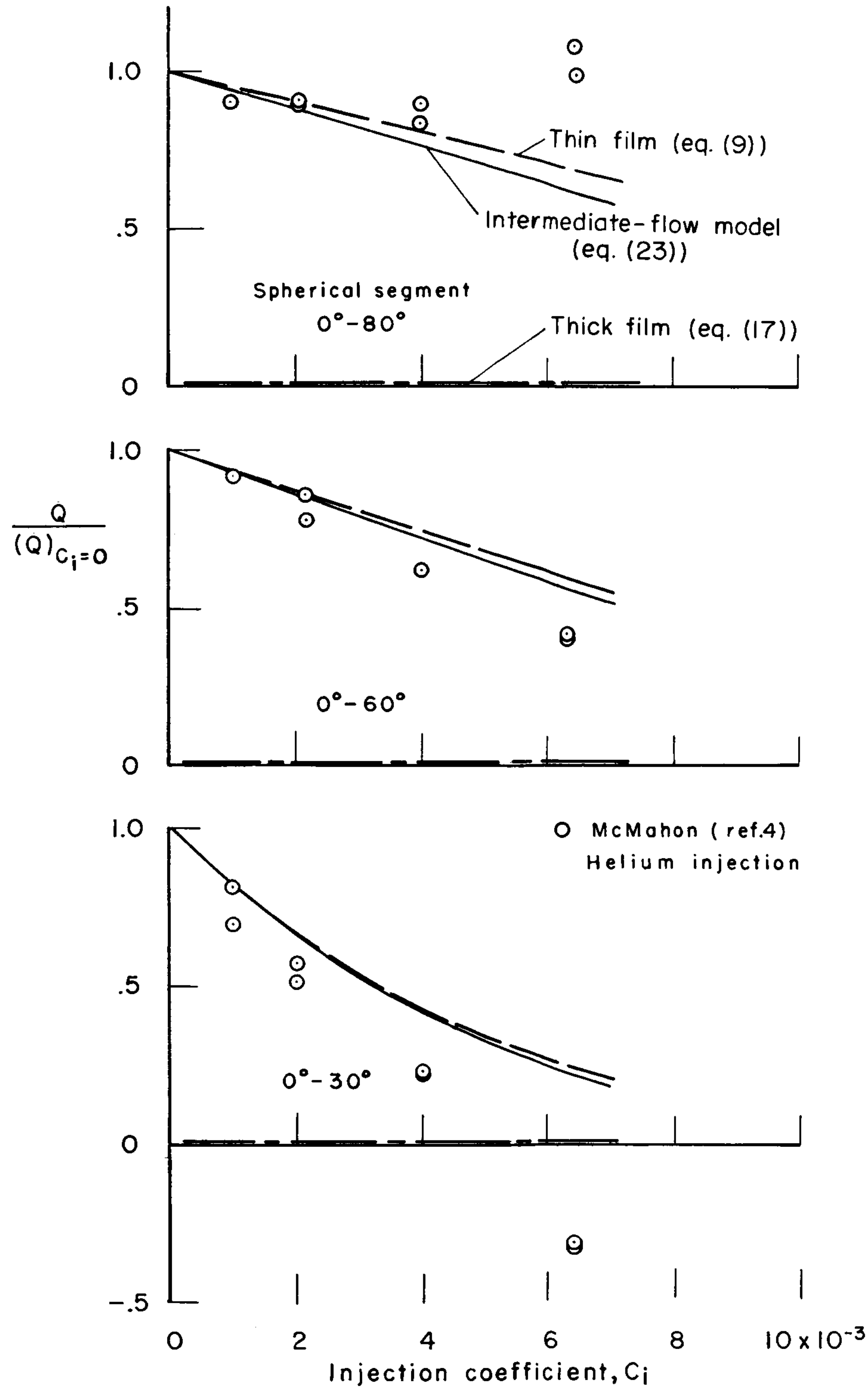

Figure 1.- Comparison of predictions with present theory with existing experimental results (helium injection).

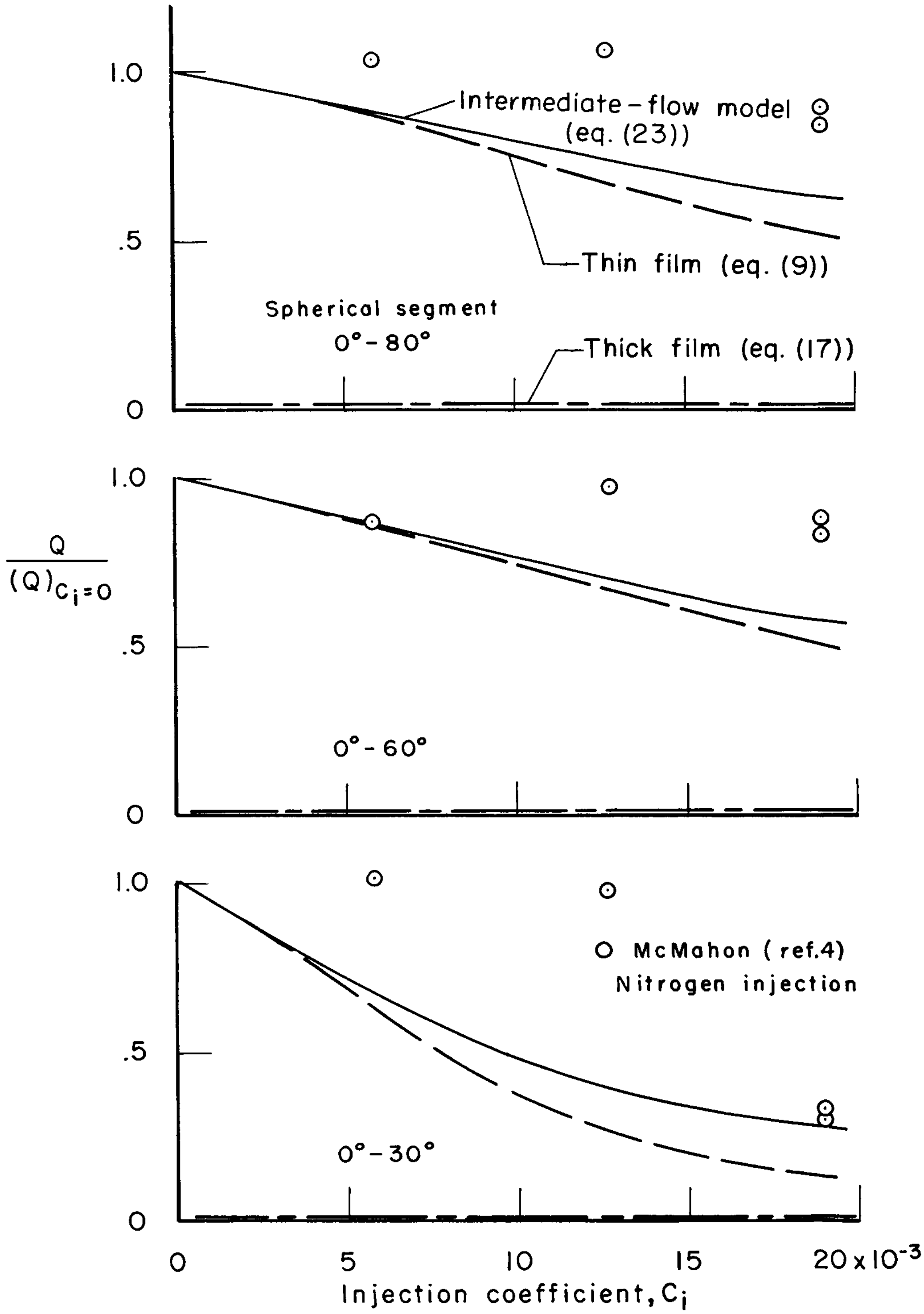

Figure 2.- Comparison of predictions with present theory with existing experimental results (nitrogen injection).

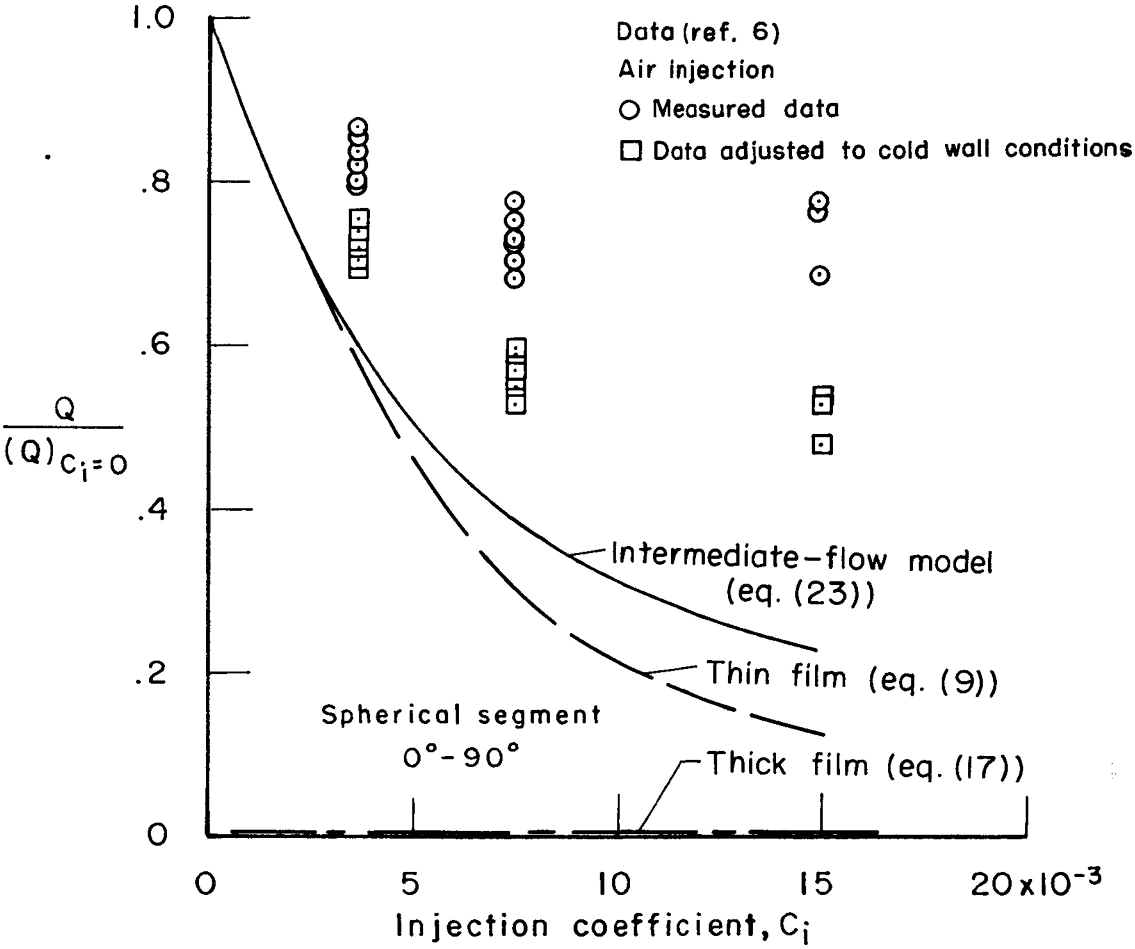

Figure 3.- Comparison of predictions with present theory with existing experimental results (air injection).

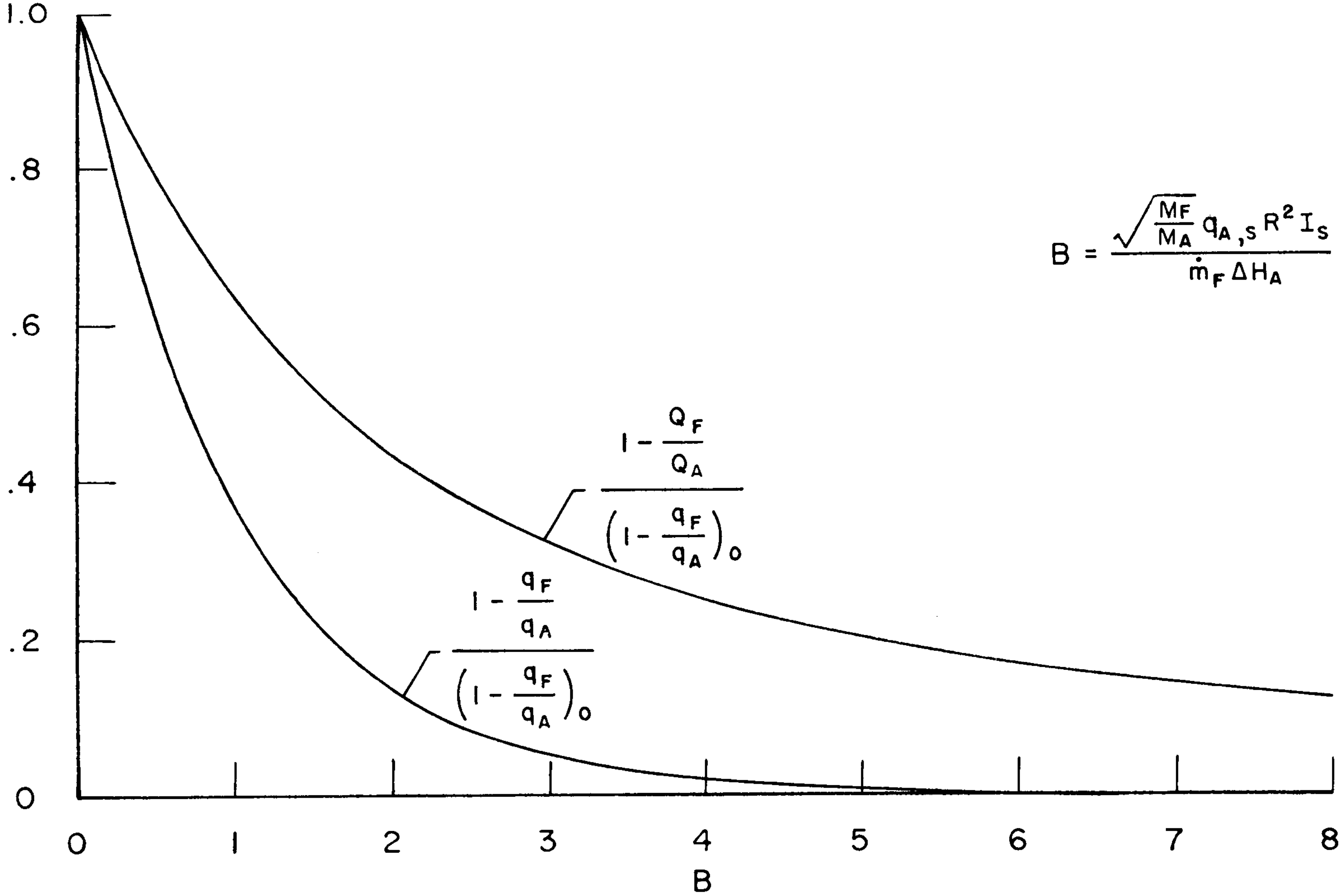

Figure 4.- Reduction in local and integrated heating rates as function of the distribution parameter B.

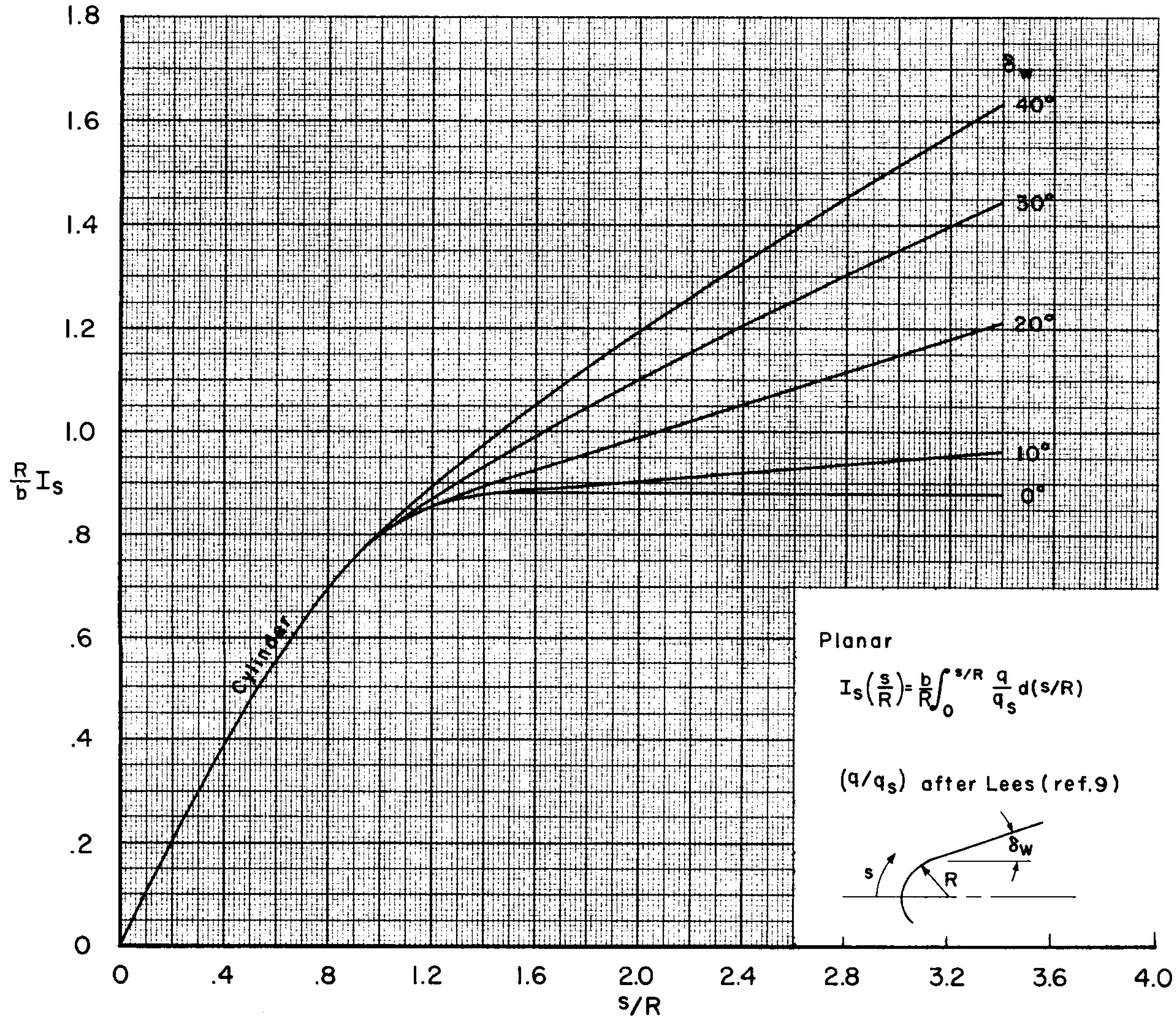

Figure 5.- Weighted surface area integral for blunted wedges.

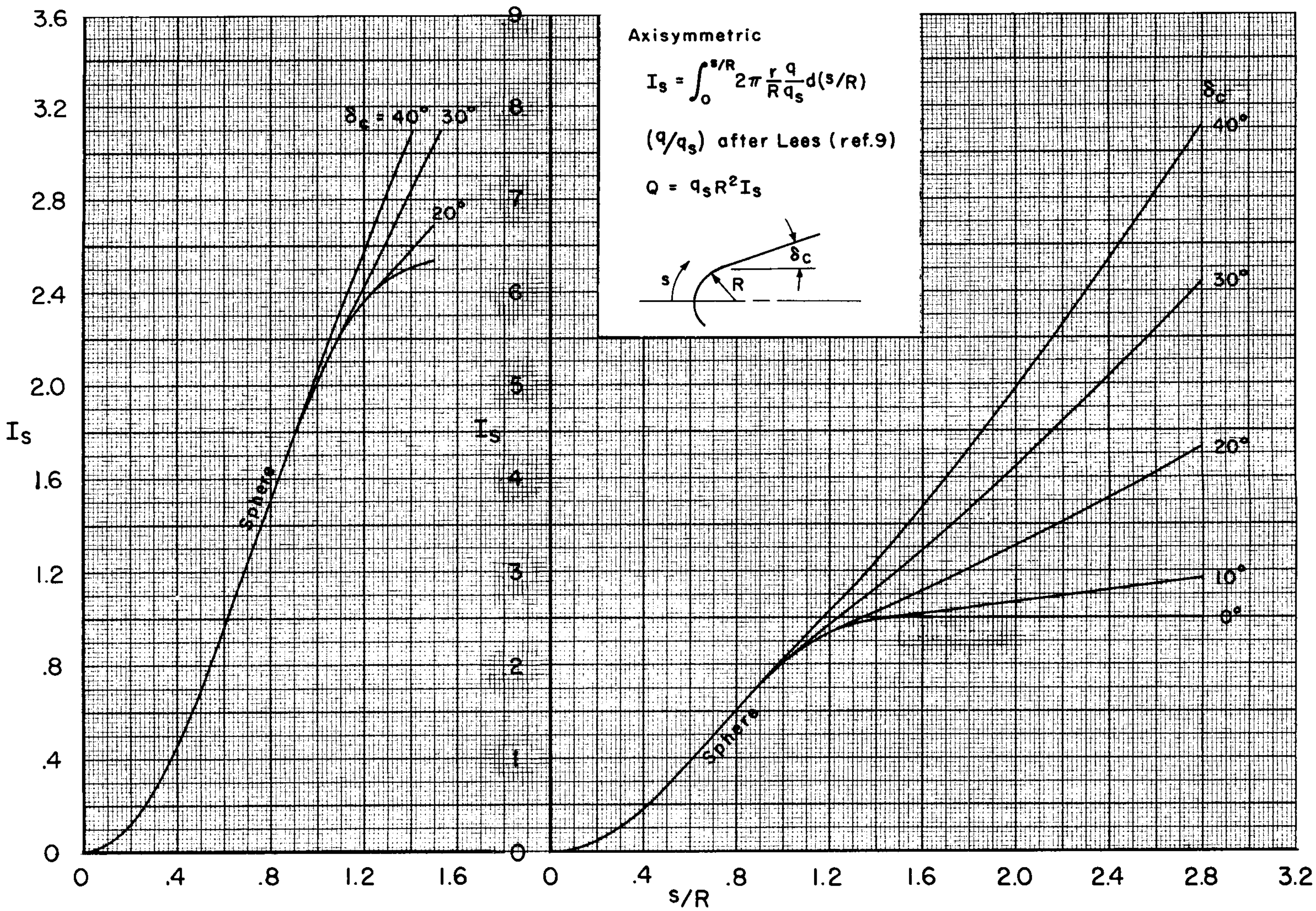

Figure 6.- Weighted surface area integral for blunted cones.

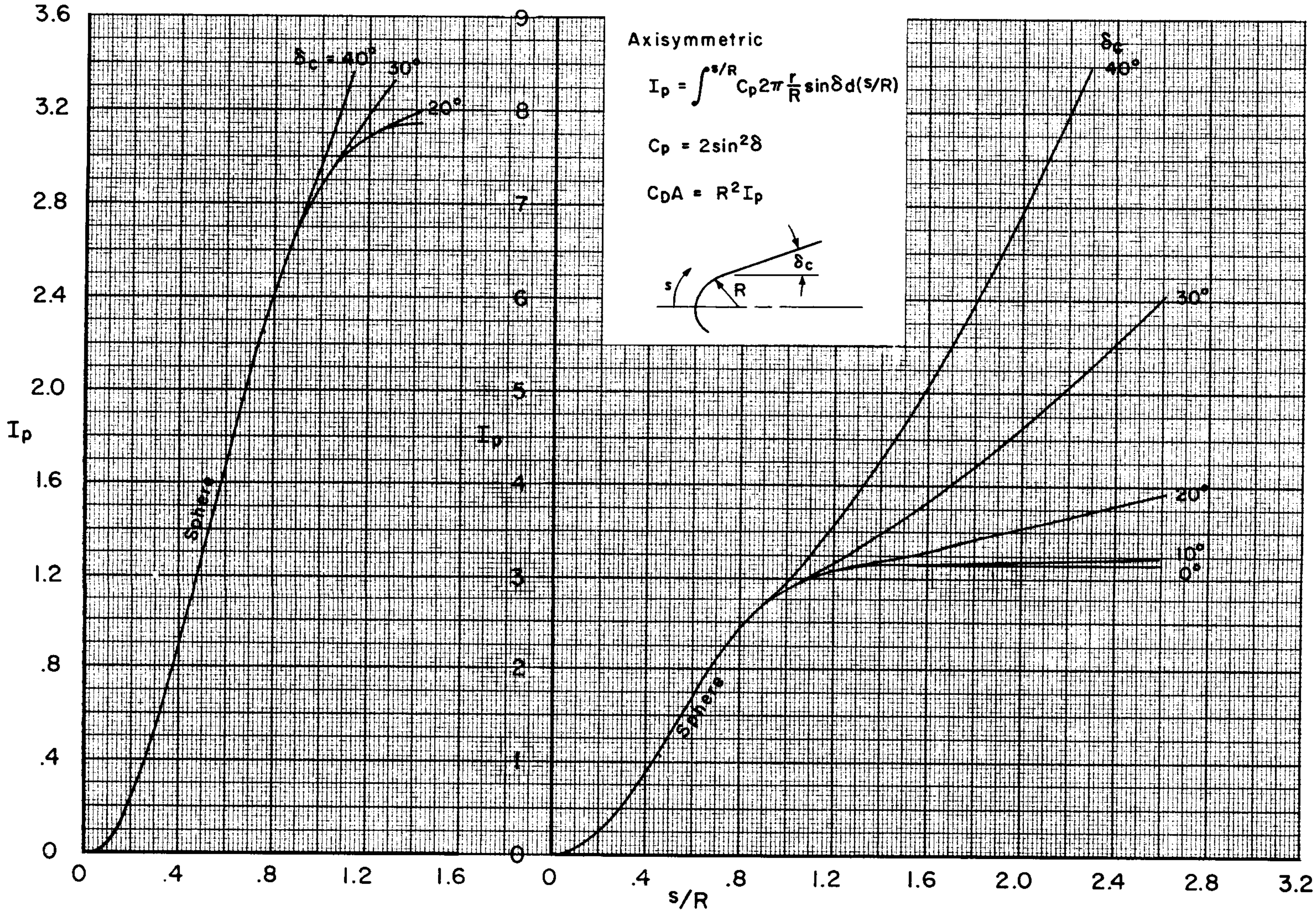

Figure 7.- Drag surface integral for blunted cones.

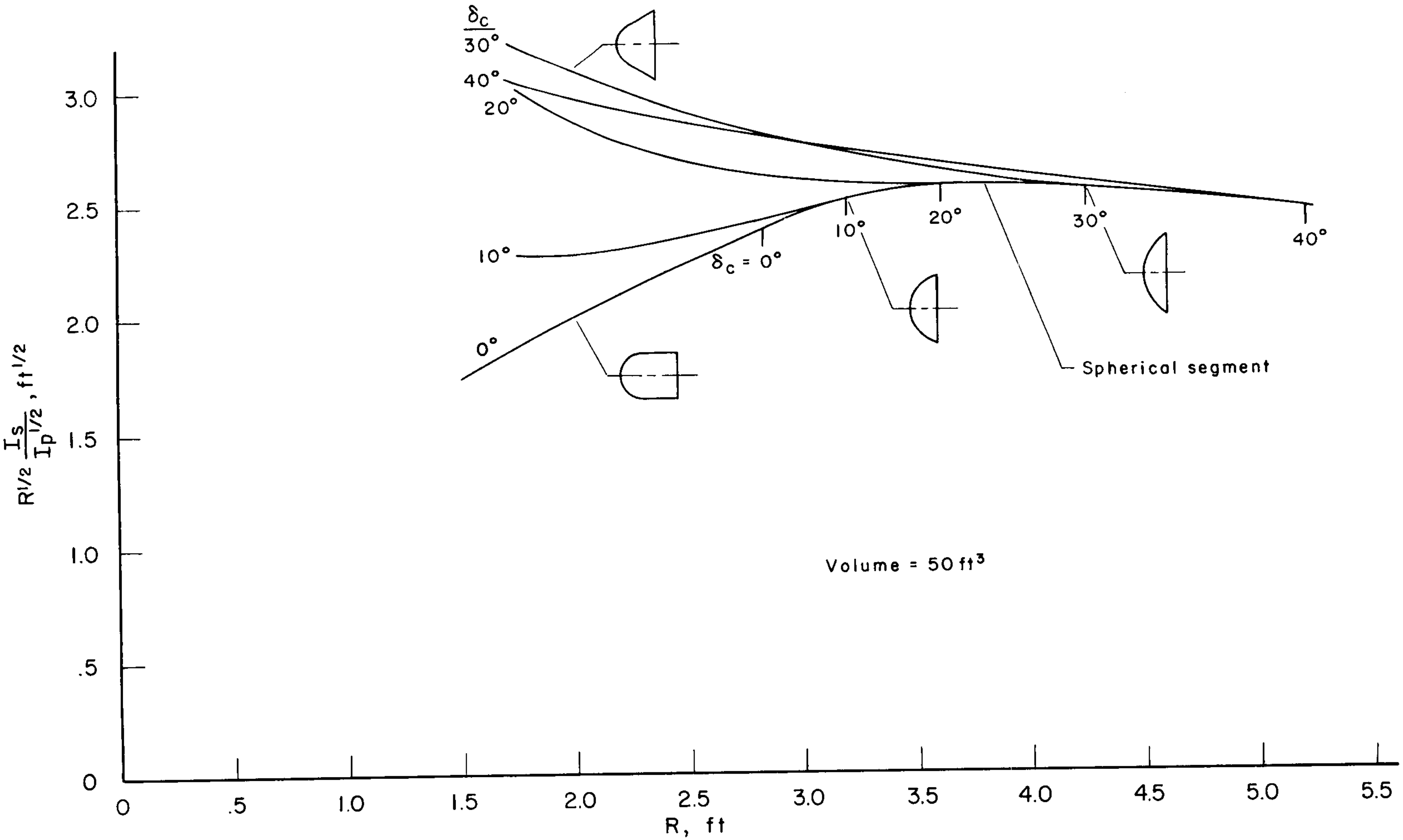

Figure 8.- Heating-rate parameter for blunted cones with a volume of 50 ft^3.

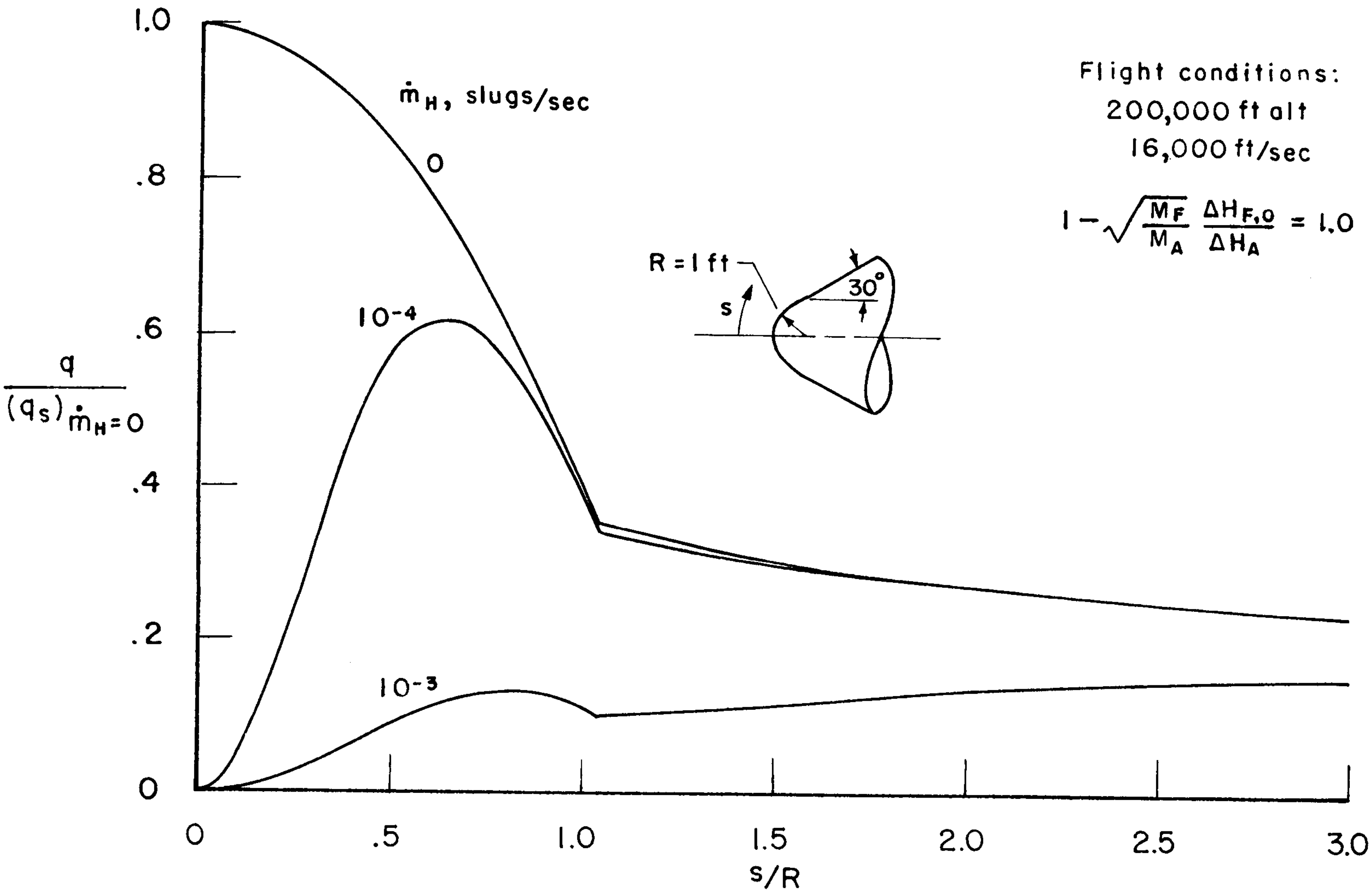

(a) Effect of mass rate of injection.

Figure 9.- Example of heating-rate distribution with helium injection.

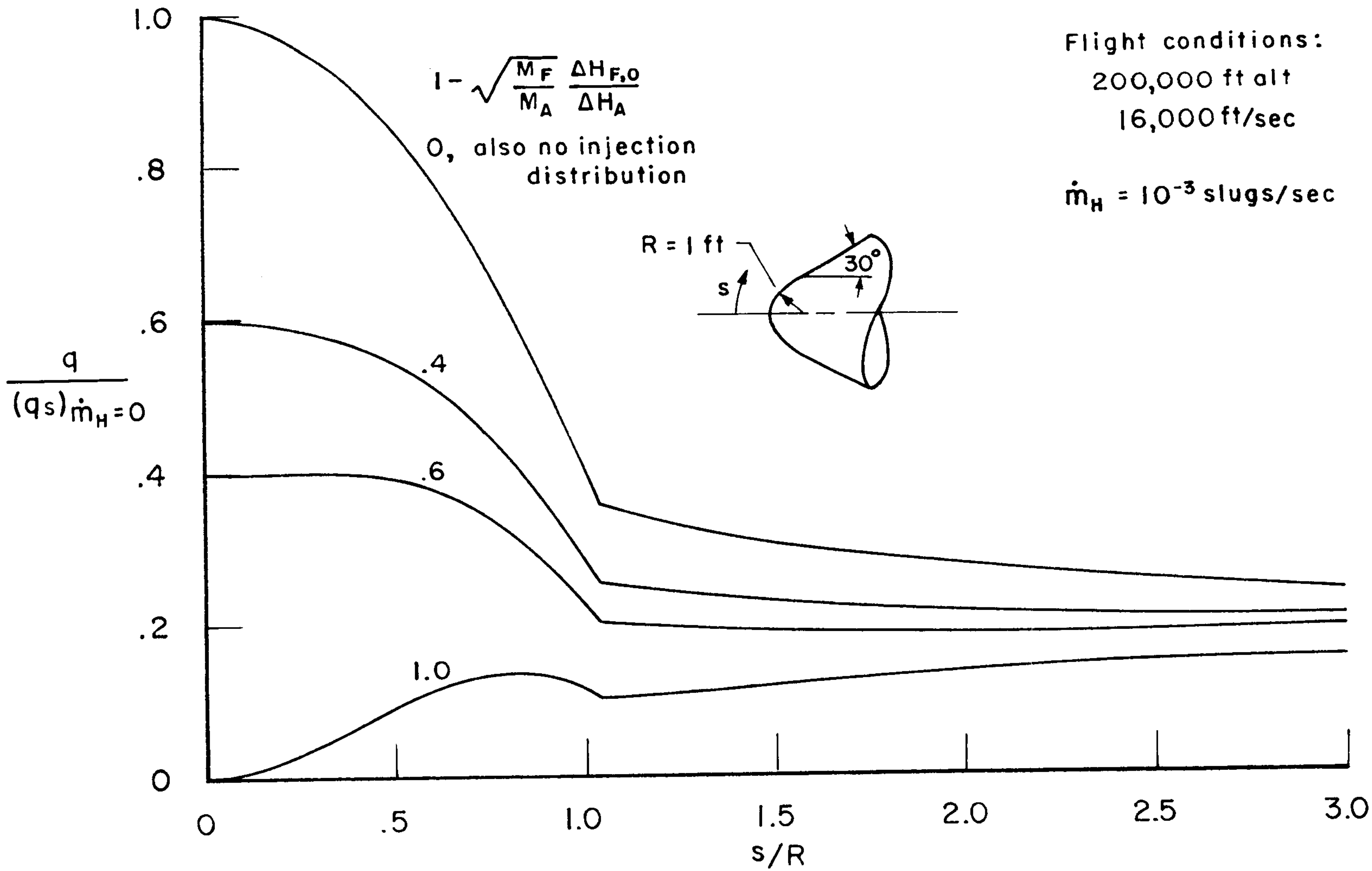

(b) Effect of injection parameter.

Figure 9.- Continued.

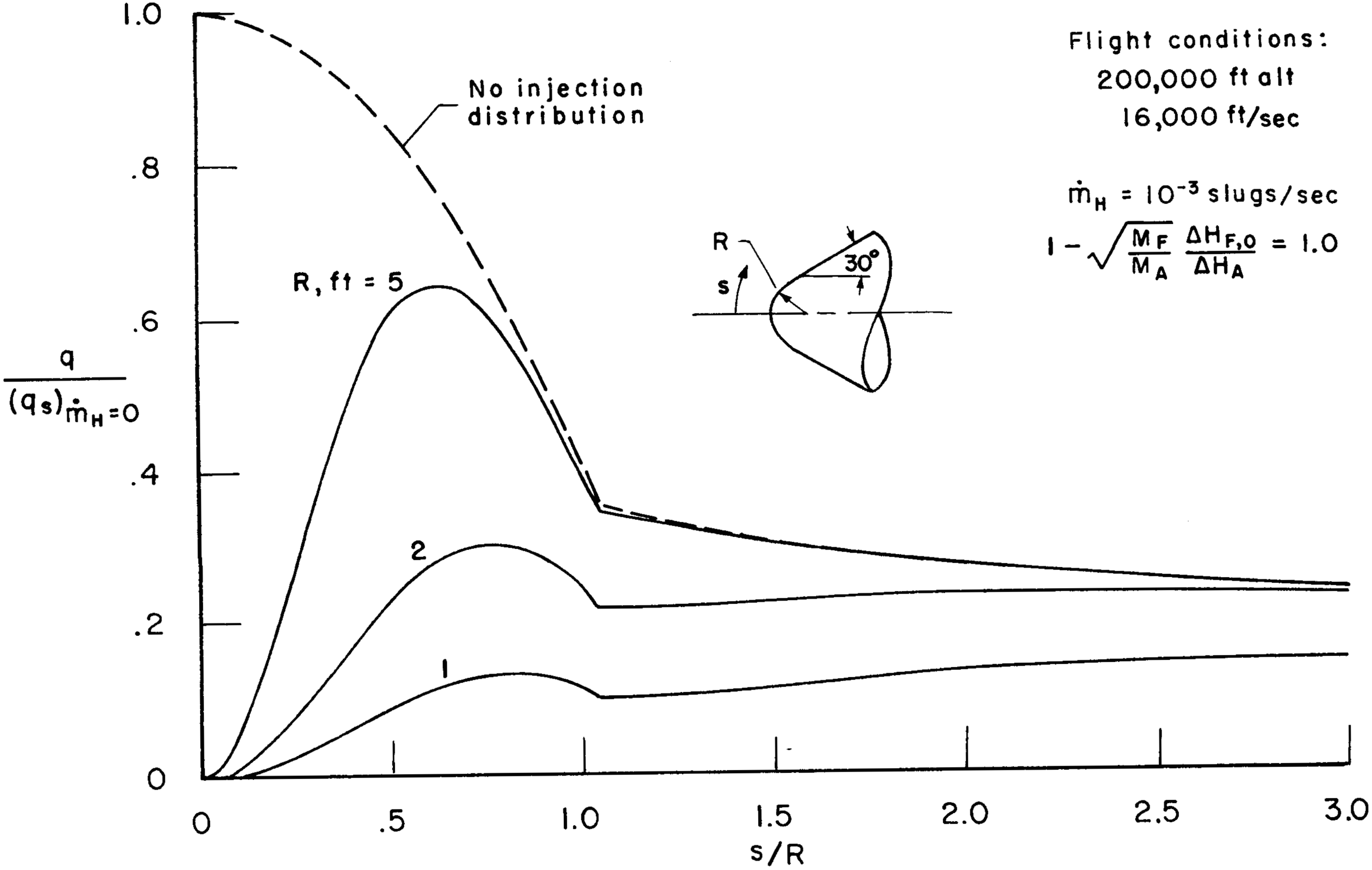

(c) Effect of nose radii.

Figure 9.- Concluded.

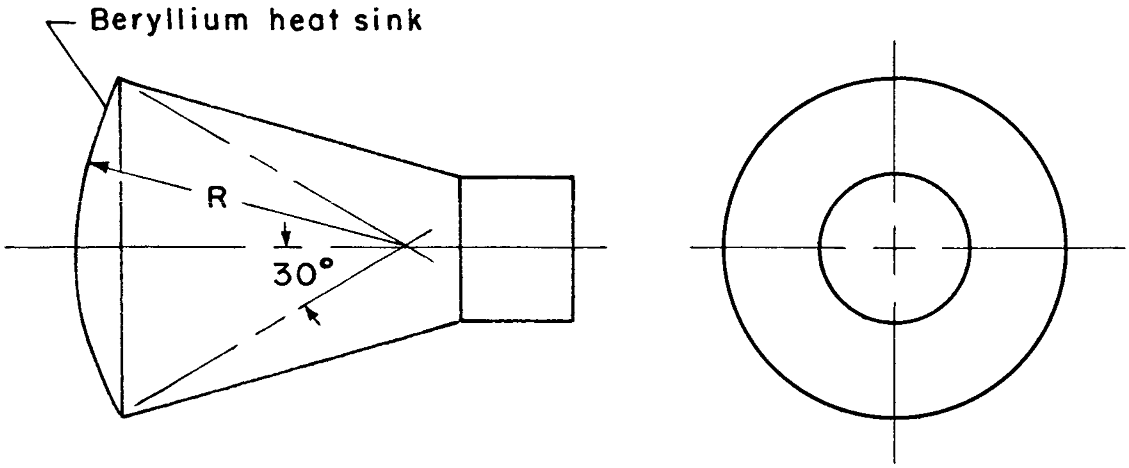

Figure 10.- Example entry configuration.

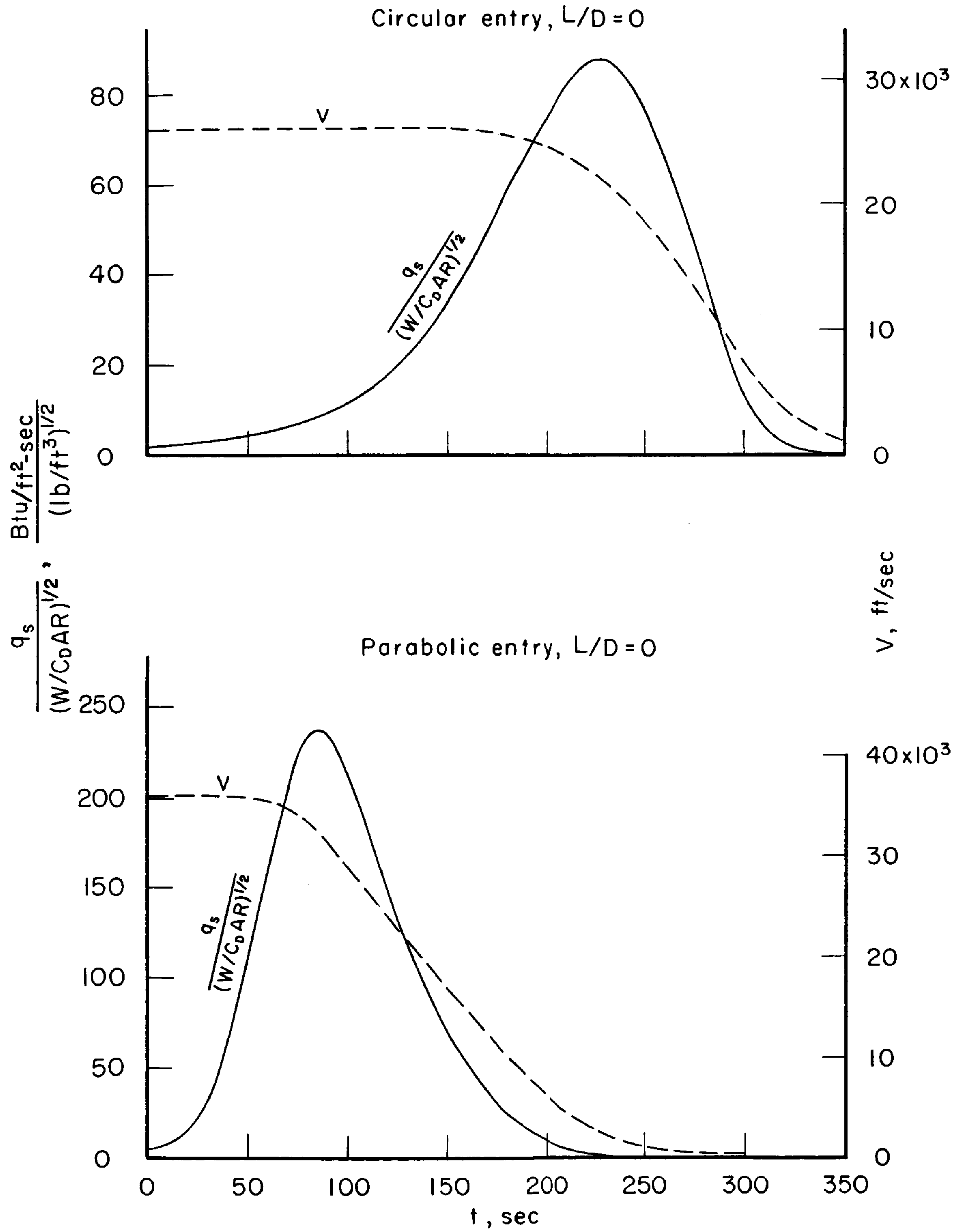

Figure 11.- Normalized heating rate and velocity histories for the example entries.